Chapter 8
Resonant Analysis of Systems Equipped with Nonlinear Displacement-Dependent (NDD) Dampers

Javad Jahanpour, Shahab Ilbeigi, and Mojtaba Porghoveh

Abstract Resonant analysis of a vibration system equipped with a nonlinear displacement-dependent (NDD) damper is investigated. The frequency of the external forcing is chosen to be close to the natural frequency of the system. The system is modeled and the approximate analytical solution of the governing equation is developed using the multiple scales method (MSM). Several case studies with various amounts of external force's frequencies are performed to investigate the resonant excitation analysis. The proposed analytical solution is also verified by the fourth order Runge-Kutta method. Moreover, the performance of the used NDD damper is analyzed and compared with the ordinary linear damper through the same periodic resonant excitation. It is found that the NDD damper has a superior performance in reducing the vibration amplitude, compared to the traditional linear damper when resonance occurs. In addition, utilizing the NDD damper in the resonant-excited system provides a smaller force transmitted to the base than the system with the ordinary linear damper.

Keywords Resonant analysis • Nonlinear displacement-dependent (NDD) damper • Periodic excitation • Multiple scales method (MSM) • Vibration amplitude reduction

8.1 Introduction

In general, to perform the vibration analysis on a system, its response under free and forced vibration is to be investigated. In free vibration analysis, the system oscillates without being subjected to forcing from the surrounding environment. While, under the forced vibrations, the system is excited by the continuously applied, time-dependent external forces which act on the system [1]. Most often these are periodic forces.

In many applications, vibration may cause discomfort, disturbance, and damage. In particular, with the forced vibration, when the external excitation frequency tends the natural frequency of the system, destruction of the system or the structure may occur [2, 3]. This phenomenon is named as resonance, which is a well-known concept in forced vibration problems. In an ideal resonance, when the frequency of an exciting force matches the natural frequency of the system; the amplitude of vibration is considerably increased. The study of resonance is an important issue in many applications such as: vehicle design [4], steam-turbine rotor-bearing systems [5], wind turbines [6, 7], bridge design [8], controllers and isolators design [9], beams [10–17], CNC tool-path planning [18] and tuned liquid damper (TLD) as an absorber [19, 20]. Also, understanding resonances is essential to ensure an appropriate running condition and a desired behavior of systems. Most studies of resonance assume that the system is linear. However, most of dynamical systems have nonlinear components, which cannot be described by a linear model. For example, vibration components with clearances [21, 22], motion limiting stops [23, 24], vibration analysis of the milling process [25], vibration modes with internal resonance [26], or a nonlinear displacement-dependent (NDD) damper [27], which cause changes in damping coefficients, represent a significant proportion of these systems.

In order to avoid the undesired effects of the resonance in both linear and nonlinear systems, different kinds of viscous dampers are added to the vibratory system. Dampers absorb the energy and do not allow the vibration amplitude to reach the infinity in resonance phase, while in conservative systems without any damper; the amplitude reaches infinity when resonance happens. Most of viscous dampers have a constant damping coefficient, however, variable dampers have already found their way to industrial/commercial applications [28, 29]. The variable dampers can be classified as active, semiactive

J. Jahanpour • M. Porghoveh
Department of Mechanical Engineering, Mashhad Branch, Islamic Azad University, Mashhad, Iran

S. Ilbeigi (✉)
Department of Mechanical, Industrial, and Systems Engineering, University of Rhode Island, Kingston, RI 02881, USA
e-mail: ilbeigi@uri.edu

G. Kerschen (ed.), *Nonlinear Dynamics, Volume 1*, Conference Proceedings of the Society for Experimental Mechanics Series,
DOI 10.1007/978-3-319-29739-2_8

and passive [30–34]. Active dampers are activated by an external source of power which usually is provided by hydraulic actuators [35–37]. In most cases, the active dampers have high energy consumption, heavy weight, large size and high cost. Semiactive dampers inherit properties of controllable electromagnetic valves or magneto rheological (MR) fluid to control the damping characteristics of the system and they are a compromise between the active and passive dampers [29–38]. Passive dampers have generally fixed properties which are determined and preset according to the design goals and intended application [38]. Even though the active and semiactive dampers have higher performance, passive dampers are still the most commonly used ones [29].

While there are many types of passive dampers, the passive variable dampers have been recently developed. Among the passive variable dampers, those with stroke and displacement/position dependent sensitivity have been studied in several works [39–50]. Fukushima et al. [43] suggested that dampers should have a stroke dependent characteristic; such that for a given velocity, a longer stroke would give a greater force. However, the force in the stroke sensitivity cannot be identified directly with the actual position of the piston in the cylinder [28]. The displacement sensitive dampers have been used on aircraft landing gear, motorcycles, and vehicle suspension applications. The displacement sensitive schemes for landing gears employ positive recoil control or two and three level position dependent damping [32]. In a motorcycle front fork, a short and blunt rubber as a needle causes the damper orifice to get closed which allows weaker springing with improved ride quality pressure [28]. Etman et al. [45] designed a stroke dependent damper for the front axle suspension of a truck. The displacement sensitive damper suggested for vehicle suspension applications follows the idea of using a long tapered needle entering an orifice in the piston [16, 34]. This type of damper is merely limited to utilizing a tapered needle and is not mathematically modeled. Lee and Moon [47, 48] reported on tests of a displacement sensitive damper with a longitudinally grooved pressure cylinder to relax the damping around the central position.

Some researchers have also investigated thoroughly the nonlinear dampers [27, 34, 49]. For instances, Haque et al. [50] proposed an integral formulation to obtain the damping force of a displacement sensitive nonlinear damper. This method was based on the transformation of the displacement sensitivity characteristic of the damper into a velocity sensitivity characteristic. Farjoud et al. [51] presented a nonlinear model of monotube hydraulic dampers with an emphasis on the effects of shim stack on damper performance. Guo et al. [52] studied the force and displacement transmissibility of nonlinear viscous damper based vibration isolation. Peng et al. [53] investigated resonant phenomena for a class of nonlinear systems using the Nonlinear Output Frequency Response Functions (NOFRFs).

Free and forced vibration analyses of systems equipped with nonlinear damper have also been studied in several researches [27, 54–57]. For instances, Bugra et al. [55] implemented several experiments to determine the dynamic characterization of nonlinear oil-free wire mesh dampers. To this end, the free and forced vibrations were investigated using the Hilbert transform procedure and controlled amplitude single frequency excitation tests, respectively. Main and Jones [56] demonstrated the free vibration of a taut cable with a nonlinear amplitude dependent damper. Diotallevi et al. [57] proposed a simplified design method to analyze the forced vibration of single- and Multi-degrees of freedom (SDF and MDF) systems equipped with nonlinear viscous damper under harmonic external forces. In their work, the responses of the SDF and MDF systems were also calculated numerically.

Recently, Ilbeigi et al. [27, 58] introduced a novel scheme for NDD dampers, in which the damping coefficient and damping force were both continuous and smooth functions of displacement. In contrast with a linear damper, where the damping force only depends on the velocity, the damping force produced by the proposed NDD damper depends on the position of the system as well as the velocity. In their work, the vibratory mass-spring system equipped with a NDD damper was also mathematically modeled and free vibration analysis of the system was analyzed. The results presented in [27] indicate that the advised passive NDD damper scheme is capable to reduce the free vibration amplitude rather than the existing traditional linear damper.

In this paper, resonant analysis of a mass-spring system utilizing the NDD damper is presented. The nonlinear differential equation of the system under an external force with the frequency close to the natural frequency of the system is derived. To study the resonance vibration analysis of the system, the external excitation's frequency is described using a detuning parameter presenting the closeness of the external force's frequency to the natural frequency of the system. The stationary response of the system is elaborated using the multiple scales method (MSM). The rest of the paper is organized as follows. Section 8.2 is a review on the NDD damper mechanism. In Sect. 8.3, the mathematical model of the nonlinear mass-spring system equipped with the NDD damper under an external resonant-force excitation is formulated and the governing differential equation is derived. The forced-resonant vibration analysis of the system is illustrated in the Sect. 8.4. Several numerical examples are presented in Sect. 8.5. The results are analyzed and discussed in Sect. 8.6. Finally, Sect. 8.7 concludes the paper.

8.2 Review on the NDD Damper Mechanism

An ordinary simple viscous damper consists of a piston having one or more orifices moving inside a cylinder filled with a viscous fluid (Fig. 8.1). The damping force produced by a damper is linearly related as follows:

$$F = -c\frac{du}{dt} \tag{8.1}$$

In which c is the damping coefficient.

By taking advantages of Hagen–Poiseuille equation for laminar flows, c can be obtained by the following equation for the case of piston with one orifice:

$$c_{linear} = \hbar\left[\left(\frac{D}{d}\right)^2 - 1\right]^2 \tag{8.2}$$

where, D and d are the cylinder diameter and the opening fluid gap diameter, respectively. Also, $\hbar = 8\pi\mu L$, in which, μ denotes for dynamic viscosity of the fluid and L is the piston width.

For a set of chosen parameters D, d and L, the damping coefficient has a constant value. The mechanism can be designed to make the linear damper into nonlinear and displacement-dependent one. To this end, [15] proposed a solid cone shaped generated by rotating the interior region of the following function in Cartesian r-u coordinates around the $u-$ axis:

$$u = nr^s \text{ or } r = \left(\frac{u}{n}\right)^{\frac{1}{s}} \tag{8.3}$$

where, $\beta = \frac{2}{d.n^{\left(\frac{1}{s}\right)}}$ and $\gamma = \frac{D}{d}$.

The fixed cone shaped part is assembled to the linear damper, so that the origin of coordinates is located on the center of the piston, the fluid travels through its outer surface and the inner surface of the orifice (Fig. 8.2), while, the opening fluid gap is changed and the damping coefficient is consequently varied. Therefore, the ordinary linear damper with a constant damping coefficient is converted to the nonlinear damper with a variable displacement-dependent damping coefficient

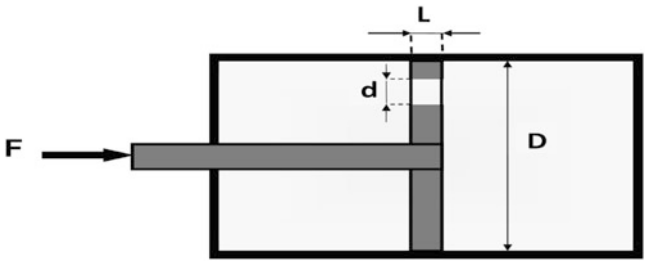

Fig. 8.1 Schematic of a simple viscous damper

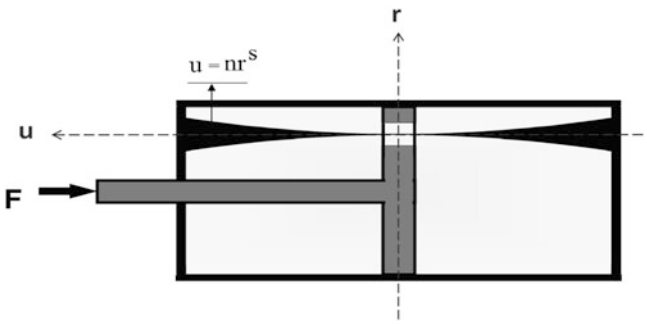

Fig. 8.2 Schematic of the nonlinear displacement-dependent (NDD) damper [27]

For the designed displacement-dependent damping mechanism shown in Fig. 8.2, the opening fluid gap diameter is equal to $d - 2r$. Substituting r from Eq. (8.3), and $d - 2r$ for d into Eq. (8.2) leads to

$$c = \hbar \left[\gamma^2 \left(\frac{1}{1 - \beta u^{\left(\frac{1}{s}\right)}} \right)^2 - 1 \right]^2 \tag{8.4}$$

where, $\beta = \frac{2}{d_n^{\left(\frac{1}{s}\right)}}$ and $\gamma = \frac{D}{d}$.

Using the 2nd-order Taylor series expansion, Eq. (8.4) can be expressed as follows [27].

$$c = \alpha_1 + \alpha_2 |u|^{\left(\frac{1}{s}\right)} + \alpha_3 |u|^{\left(\frac{2}{s}\right)} + \alpha_4 |u|^{\left(\frac{3}{s}\right)} + \alpha_5 |u|^{\left(\frac{4}{s}\right)} \tag{8.5}$$

For the case of $n = 1$ and $s = \frac{1}{2}$, Eq. (8.5) will be rewritten as follows:

$$c = \alpha_1 + \alpha_2 u^2 + \alpha_3 u^4 + \alpha_4 u^6 + \alpha_5 u^8 \tag{8.6}$$

The parameters α_i in Eq. (8.6) are given in Appendix.

It is noticed that the damping coefficient of the traditional damper is constant value, whereas the damping coefficient of a NDD damper changes as the system moves. More details on mathematical formulation of the NDD damper can be found in [15].

8.3 Mathematical Formulation of the Forced-Resonant Mass-Spring-NDD Damper System

The governing differential equation of a simple mass-spring-damper system with an external periodic force follows:

$$\ddot{u} + \frac{c}{m}\dot{u} + {\omega_n}^2 u = \frac{F \cos(\Omega t)}{m} \tag{8.7}$$

where, $\omega_n = \sqrt{\frac{k_s}{m}}$ is the natural frequency of the system, Ω is the external force's frequency and F is the excitation amplitude.

For a linear damper with constant damping coefficient, the forced-resonant response of the system is as follows:

$$\begin{aligned} u_l(t) = A_1 e^{-\zeta \omega_n t} \sin\left(\sqrt{1-\zeta^2}\omega_n t + \psi\right) \\ + A_2 \cos(\Omega t - \varphi) \end{aligned} \tag{8.8}$$

where, $\zeta = \frac{c}{2\sqrt{mk_s}}$. Also, A_1 and ψ are evaluated using initial conditions. Moreover, A_2 and φ related to the particular solution of Eq. (8.7), are given in Appendix.

The damping force and the total force transmitted to the base can be calculated by the following equations:

$$F_{\text{Damping}} = c\frac{du(t)}{dt}. \tag{8.9}$$

$$F_{\text{Transmitted}} = c\,\dot{u} + k_s\,u. \tag{8.10}$$

In order to achieve the governing differential equation of a basic mass-spring system equipped with NDD damper with an external force, c from Eq. (8.6) must be replaced into Eq. (8.7) as follows:

$$\begin{aligned} \frac{d^2u}{d\widehat{t}^2} + u = -\varepsilon\left(1 + \beta_1 u^2 + \beta_2 u^4 + \beta_3 u^6 + \beta_4 u^8\right)\frac{du}{d\widehat{t}} \\ + K\cos\left(\lambda\widehat{t}\right) \end{aligned} \tag{8.11}$$

In which, $\widehat{t} = \omega_n\, t$, $\varepsilon = \frac{\hbar\left(\gamma^4 - 2\gamma^2 + 1\right)}{m\omega_n}$, $\beta_i = \frac{\alpha_{i+1}}{\alpha_1}$, $K = \frac{F}{m{\omega_n}^2}$ and $\lambda = \frac{\Omega}{\omega_n}$.

By adding a small term to the mathematical description (ε in this paper), a perturbation method can be used to find an approximate solution to the governing differential Eq. (8.11). The parameter ε is directly proportional to $\hbar$ and, accordingly, to the fluid viscosity. It is also dependent to γ. Hence, increasing the viscosity or increasing γ, causes increasing ε, and strength of nonlinearity in Eq. (8.11), successively.

The shape parameters, i.e. n and s, effect on β as $\beta = \frac{2}{d_c n^{\frac{1}{s}}}$ and successively on the damping coefficient c as given by Eq. (8.4). Accordingly, the dimensionless form of the governing equation of the vibration system utilizing the NDD damper with an external periodic excitation is affected by these shape parameters (see Eq. (8.11)). It should be noted that the values of the shape parameters n and s do not have any effect on ε the one parameter which describes the strength of nonlinearity of the governing equation. Since the main focus of this paper is to analyze forced-resonant vibration of a system equipped with NDD damper, the shape parameters have been selected as a fixed set for a general application. However, the couple of the values of these parameters can be optimized according to the desire goal and intended particular application.

For the forced-resonant analysis of the mass-spring-NDD damper system, the excitation frequency is considered as:

$$\Omega = \omega_n + \delta\varepsilon \tag{8.12}$$

where, δ is the detuning parameter to present the deviation of the external force's frequency from the natural frequency of the system. Also, the external force amplitude coefficient, i.e. K, can be expressed as $K = \varepsilon k$ without any loss of the generality of the mathematical model. Therefore, the term related to the periodic-resonant external force in Eq. (8.11) can be expressed as following equation:

$$K\cos\left(\lambda\widehat{t}\right) = \varepsilon k\cos\left[\widehat{t} + \frac{\varepsilon\delta}{\omega_n}\widehat{t}\right] \tag{8.13}$$

Substituting Eq. (8.13) in Eq. (8.11) leads to:

$$\begin{aligned}\frac{d^2u}{d\widehat{t}^2} + u = -\varepsilon\left(1 + \beta_1 u^2 + \beta_2 u^4 + \beta_3 u^6 + \beta_4 u^8\right)\frac{du}{d\widehat{t}} + \\ \varepsilon k\cos\left[\widehat{t}\left(1 + \frac{\varepsilon\delta}{\omega_n}\right)\right]\end{aligned} \tag{8.14}$$

where, $\beta_i = \frac{\alpha_{i+1}}{\alpha_1}$ are given in Appendix.

In the following section, the procedure of employing MSM as a perturbation technique is illustrated to solve Eq. (8.14).

8.4 Forced-Resonant Vibration Analysis of the Mass-Spring-NDD Damper Using MSM

This method is based on the idea of representing multiple independent variables, which are all functions of the time variable, and express all other time dependent functions including the response, as functions of the represented variables [54, 59–61]. For this aim, the independent variables are introduced as:

$$T_n = \varepsilon^n\widehat{t} \quad \text{for} \quad n = 0, 1, 2, 3 \tag{8.15}$$

Thus, the term related to the periodic-resonant external force in Eq. (8.14) can be determined using the terms T_0 and T_1 as follows

$$\varepsilon k\cos\left[\widehat{t}\left(1 + \frac{\varepsilon\delta}{\omega_n}\right)\right] = \varepsilon k\cos\left(T_0 + \frac{\delta}{\omega_n}T_1\right) \tag{8.16}$$

Assuming $n = 0$ and 1, the solution of Eq. (8.14) can be expressed as

$$u = u_0\left(T_0, T_1\right) + \varepsilon u_1\left(T_0, T_1\right) + O\left(\varepsilon^2\right) \tag{8.17}$$

With regard to the chain rule of derivation, the first and second derivatives with respect to $\widehat{t}$ can be represented as the following forms:

$$\begin{aligned}\frac{d}{d\widehat{t}} &= D_0 + \varepsilon D_1 \\ \frac{d^2}{d\widehat{t}^2} &= D_0^2 + 2\varepsilon D_0 D_1 + \varepsilon^2 D_1^2\end{aligned} \tag{8.18}$$

where $D_n = \frac{\partial}{\partial T_n}$.

Substituting Eqs. (8.16), (8.17), and (8.18) into Eq. (8.14) and equating coefficient of each power of ε in the two sides of equation together, leads to

$$D_0^2 u_0 + u_0 = 0 \tag{8.19}$$

$$\begin{aligned}D_0^2 u_1 + u_1 = -2D_0 D_1 u_0 - \Big(1 + \beta_1 u_0^2 + \\ \beta_2 u_0^4 + \beta_3 u_0^6 + \beta_4 u_0^8\Big) D_0 u_0 + k\cos\left(T_0 + \tfrac{\delta}{\omega_n} T_1\right).\end{aligned} \tag{8.20}$$

Assuming $\eta = \frac{\delta}{\omega_n}$, then, the term $k\cos\left(T_0 + \frac{\delta}{\omega_n} T_1\right)$ in Eq. (8.20) can be rewritten as:

$$\begin{aligned}k\cos\left(T_0 + \eta T_1\right) &= \tfrac{k}{2}\left[e^{i(T_0+\eta T_1)} + e^{-i(T_0+\eta T_1)}\right] \\ &= \tfrac{k}{2} e^{i\eta T_1}.e^{iT_0} + \tfrac{k}{2} e^{-i\eta T_1}.e^{-iT_0}\end{aligned} \tag{8.21}$$

The general solution of Eq. (8.19) can be expressed as

$$u_0 = A\left(T_1\right)\ e^{iT_0} + \overline{A}\left(T_1\right)\ e^{-iT_0} \tag{8.22}$$

Substituting for u_0 from Eq. (8.22) and the term related to the external force from Eq. (8.21) into Eq. (8.20) gives

$$\begin{aligned}{D_0}^2 u_1 + u_1 = -i\Big[\Delta_s e^{iT_0} + \Delta_3 e^{3iT_0} + \Delta_5 e^{5iT_0} \\ + \Delta_7 e^{7iT_0} + \Delta_9 e^{9iT_0} + \mathrm{CC}\Big].\end{aligned} \tag{8.23}$$

In which,

$$\begin{aligned}\Delta_s = 2D_1 A + A + \beta_1 A^2\overline{A} + 2\beta_2 A^3\overline{A}^2 + \\ 5\beta_3 A^4\overline{A}^3 + 14\beta_4 A^5\overline{A}^4 - \tfrac{1}{2} ike^{i\eta T_1}\end{aligned} \tag{8.24}$$

Also, Δ_i ' s are given in Appendix and CC stands for complex conjugate.

Omitting the terms that produce secular terms leads to solvability for the first-order approximation, therefore, the coefficients of $e^{\pm iT_0}$ must be vanished; that is

$$\Delta_s = 0 \tag{8.25}$$

Thus

$$\begin{aligned}-2D_1 A = A + \beta_1 A^2\overline{A} + 2\beta_2 A^3\overline{A}^2 + \\ 5\beta_3 A^4\overline{A}^3 + 14\beta_4 A^5\overline{A}^4 - \tfrac{1}{2} ike^{i\eta T_1}\end{aligned} \tag{8.26}$$

In order to solve Eq. (8.26) and for omitting the secular terms one let

$$A = \frac{1}{2}a\left(T_1\right)\ e^{i\phi(T_1)} \tag{8.27}$$

Substituting Eq. (8.27) and its conjugate and derivatives into Eq. (8.26) and separating the imaginary and real parts leads to

$$\begin{aligned}&\tfrac{da}{dT_1} = -a - \tfrac{1}{4}\beta_1 a^3 - \tfrac{1}{8}\beta_2 a^5 - \tfrac{5}{64}\beta_3 a^7 - \\ &\tfrac{7}{128}\beta_4 a^9 + k\sin\left(-\phi + \eta T_1\right)\end{aligned} \tag{8.28a}$$

$$\frac{d\phi}{dT_1} = -\frac{k\cos\left(-\phi + \eta T_1\right)}{a} \tag{8.28b}$$

To eliminate the explicit time dependence of the right-hand sides of (8.28a) and (8.28b) one let

$$\psi = \eta T_1 - \phi \tag{8.29a}$$

Or

$$\frac{d\psi}{dT_1} = \eta - \frac{d\phi}{dT_1} \tag{8.29b}$$

Hence (8.28a) and (8.28b) can be rewritten as follows

$$\begin{aligned}&\tfrac{da}{dT_1} = -a - \tfrac{1}{4}\beta_1 a^3 - \tfrac{1}{8}\beta_2 a^5 - \tfrac{5}{64}\beta_3 a^7 - \\ &\tfrac{7}{128}\beta_4 a^9 + k\sin\left(\psi\right)\end{aligned} \tag{8.30}$$

$$\frac{d\psi}{dT_1} = \eta + \frac{k\cos\left(\psi\right)}{a} \tag{8.31}$$

Periodic solution of the externally excited system correspond to the stationary solutions of Eqs. (8.30) and (8.31), where both a and ψ become constant, that is

$$\frac{da}{dT_1} = 0 \tag{8.32}$$

$$\frac{d\psi}{dT_1} = 0 \tag{8.33}$$

Suppose $\tilde{a}$ and $\tilde{\psi}$ refer to the stationary solution of a and ψ, thus Substituting (8.30) and (8.31), respectively in (8.32) and (8.33), results in

$$\begin{aligned}&\tilde{a} + \tfrac{1}{4}\beta_1\tilde{a}^3 + \tfrac{1}{8}\beta_2\tilde{a}^5 + \tfrac{5}{64}\beta_3\tilde{a}^7 + \tfrac{7}{128}\beta_4\tilde{a}^9 \\ &- k\sin\left(\tilde{\psi}\right) = 0\end{aligned} \tag{8.34a}$$

$$\eta + \frac{k\cos\left(\tilde{\psi}\right)}{\tilde{a}} = 0 \tag{8.34b}$$

Elimination $\tilde{\psi}$ from (8.34a) and (8.34b) leads to the following algebraic equation, which describes the stationary amplitude response of the resonant excited system.

$$\tilde{a}^2 \frac{\delta}{\omega_n^2}^2 + \left(\tilde{a} + 0.25\beta_1\tilde{a}^3 + \frac{1}{8}\beta_2\tilde{a}^5 + \frac{5}{64}\beta_3\tilde{a}^7 + \frac{7}{128}\beta_4\tilde{a}^9\right)^2 = k^2 \tag{8.35}$$

For a given set of excitation amplitude and frequency, the stationary amplitude response of the resonant excited system, i.e. $\tilde{a}$ is computed via Eq. (8.35).

Substituting A from Eq. (8.27) into Eq. (8.22), the following first approximation to the response of the excited system is obtained as

$$u = a\cos\left(\widehat{t} + \phi\left(\widehat{\varepsilon t}\right)\right) + O(\varepsilon) \tag{8.36}$$

The frequency of the above periodic-resonant response of the system is determined as follows.

$$\begin{aligned}\omega = \frac{d}{dt}\left(\widehat{t} + \phi\left(\widehat{\varepsilon t}\right)\right) &= \frac{d}{dt}\left(\omega_n t + \phi\left(\widehat{\varepsilon t}\right)\right) \\ &= \omega_n + \frac{d\phi\left(\widehat{\varepsilon t}\right)}{dt}\end{aligned} \tag{8.37}$$

According to Eqs. (8.29b) and (8.33), $\frac{d\phi}{dT_1}$ is obtained as

$$\frac{d\phi}{dT_1} = \eta = \frac{\delta}{\omega_n} \tag{8.38}$$

where $T_1 = \widehat{\varepsilon t} = \varepsilon\omega_n t$. Thus:

$$\frac{d\phi}{dt} = \varepsilon\delta \tag{8.39}$$

Substituting Eq. (8.39) into Eq. (8.37) leads to the frequency of the resonant response of the system, that is

$$\omega = \omega_n + \varepsilon\delta = \omega_n\lambda = \Omega \tag{8.40}$$

According to Eq. (8.40), the frequency of the response matches the external force's frequency for the periodic resonant excitation.

8.5 Numerical Examples

The system characteristics such as mass, spring stiffness, viscosity, orifice diameter, etc. affect the values of the parameters $\omega_n, \gamma, \varepsilon, \beta_1, \beta_2, \beta_3, \beta_4$ and consequently the approximate analytical response of the resonant excited system via Eq. (8.36) and its stationary amplitude via Eq. (8.35), as well. Table 8.1 exhibits the selected values for several numerical case studies of resonant-excitation with different values of deviation factor δ. According to Table 8.1, the external force's frequency has been selected to be close to the natural frequency of the system for the cases of (1)–(4). While, the deviation of the external force's frequency from the natural frequency of the system is chosen as a large value for the fifth case.

For all cases, $k_s = 1000\frac{N}{m}$, m = 20 Kg, d = 4 cm, D = 20 cm, $n = 1$, $s = \frac{1}{2}$, and L = 1 cm have been selected. Using these values, the parameters $\omega_n, \gamma, \beta_1, \beta_2, \beta_3$ and β_4 can be calculated for all cases given in Table 8.1. Those are:

$$\begin{aligned}&\omega_n = 7.071 \text{ rad/s}^{-1}, \gamma = 5, \beta_1 = 208.3, \\ &\beta_2 = 16059, \beta_3 = 542000, \beta_4 = 6782 \times 10^3\end{aligned}$$

For instance, for the fourth case of Table 8.1 with the initial conditions as: $u(0) = 0.002$ m, $\dot{u}(0) = 1.23$ ms^{-1}, $F = 50$N and $\mu = 0.0493$ Pa.s (i.e. $\hbar = 0.0123$ and $\varepsilon = 0.05$) along with $\delta = 2$, the amount of the stationary response amplitude

Table 8.1 The selected values and the affected parameters for the resonant-excitation analysis

		Selected values					Affected parameters				
Case	F (N)	μ (Pa.s)	u_0 (m)	$\dot{u}_0$ (ms^{-1})	δ	ε	$\hbar$	ζ	c_{linear} (Nsm^{-1})	Ω (rad/s^{-1})	$\tilde{a}$ (m)
1	50	0.0493	0.002	1.23	0	0.05	0.0123	0.025	7.08	7.071	0.173
2	50	0.0493	0.002	1.23	1	0.05	0.0123	0.025	7.08	7.121	0.172
3	50	0.49	0.002	0.54	1	0.5	0.59	0.25	71	7.571	0.074
4	50	0.0493	0.002	1.23	2	0.05	0.0123	0.025	7.08	7.170	0.172
5	50	0.0493	0.002	1.35	20	0.05	0.0123	0.025	7.08	8.071	0.168

for the resonant-excited system is computed as $\tilde{a} = 172.88$ mm by solving the algebraic Eq. (8.35). Also, the excitation frequency is computed as $\Omega = \omega_n + \varepsilon\delta = 7.171$ rad/s, and the response of the excited system is obtained by Eq. (8.36) as:

$$u = 172.88\cos(7.171t + 1.56) \text{ mm}$$

The response of the mass-spring system equipped with the traditional linear damper having the same external force and initial conditions is calculated as follows:

$$x = -422\cos(7.171t) + 745\sin(7.171t) + 711e^{-0.177t}\sin(7.07t + 2.50)\,\text{mm}$$

8.6 Results and Discussion

The simulation results for the resonant excitation analysis are shown in Figs. 8.3, 8.4, 8.5, and 8.6. In order to verify the accuracy of the approximate analytical response of the system equipped with the NDD damper, given by Eq. (8.36), the numerical integration technique is also applied to solve Eq. (8.14) using the fourth order Runge Kutta method.

The displacements of the excited system using the NDD damper, for the first four cases presented in Table 8.1 are shown in Fig. 8.3. These results for the system with the linear damper are also depicted in Fig. 8.3. Figure 8.3a shows the comparison between the approximate analytical solution and the numerical result obtained by the Runge Kutta method for the ideal resonant case, i.e. the first case given in Table 8.1 with $F = 50\text{N}, \delta = 0$, (i.e. $\Omega = \omega_n = 7.071$ rad/s) and $\varepsilon = 0.05$. This comparison is carried out for the cases (2)–(4) in Fig. 8.3b–d, respectively. As can be seen the proposed analytical solution is extremely close to the numerical solution for these cases as well as the ideal resonant case, i.e. case (1). As shown in Fig. 8.3a–d, the response of the system using the linear damper considerably grows in each cycle up to an extremely large stationary amplitude at a long time for the cases of (1)–(4). But, in the system with the NDD damper, the amplitude of the vibration tends to its stationary value immediately. Therefore, there is no need to evaluate the second order approximation of u for the governing equation of the system via Eq. (8.14). Besides, as it is observed in Fig. 8.3a–d, for the system employing the NDD damper, the amount of the stationary response amplitude is significantly smaller than its value for the system with linear damper. Hence, utilizing the NDD damper in the excited system under periodic-resonant force has substantial advantage over the linear damper in terms of decreasing the amplitude response of the system.

In order to investigate the effect of increasing the perturbation parameter ε, the results related to the case (2) with $\varepsilon = 0.05$ and case (3) with $\varepsilon = 0.5$ can be evaluated. According to Fig. 8.3b, c, increasing the value of ε causes increasing the error between the approximate analytical solution and the exact numerical solution. This is due to the properties of the multiple scales method, whereas the value of ε must be small. Moreover, in Fig. 8.3c, where the amount of displacement is not considerable as the other cases, the displacements of the systems with the NDD and linear damper are close to each other, because the small amplitude vibration weakens the nonlinearity of Eq. (8.16).

Figure 8.4 exhibits the damping force of the both nonlinear and linear dampers versus displacement for the first four cases of Table 8.1. That is the work done by the damper, i.e. the amount of energy absorbed by the damper. For instance, as can be seen in Fig. 8.4b, for the case (2) with $\delta = 1$, the damping force of the linear damper has the maximum value of 42.3N, whereas, the nonlinear damper provides the larger damping force amount of 114.6N. This explains how the NDD damper outclasses the traditional linear damper in the terms of amplitude reduction.

Figure 8.5 demonstrates the transmitted force to the base versus time for the cases presented in Table 8.1. According to Fig. 8.5, in the system with the linear damper, a larger amount of force is being transmitted to the base compared to

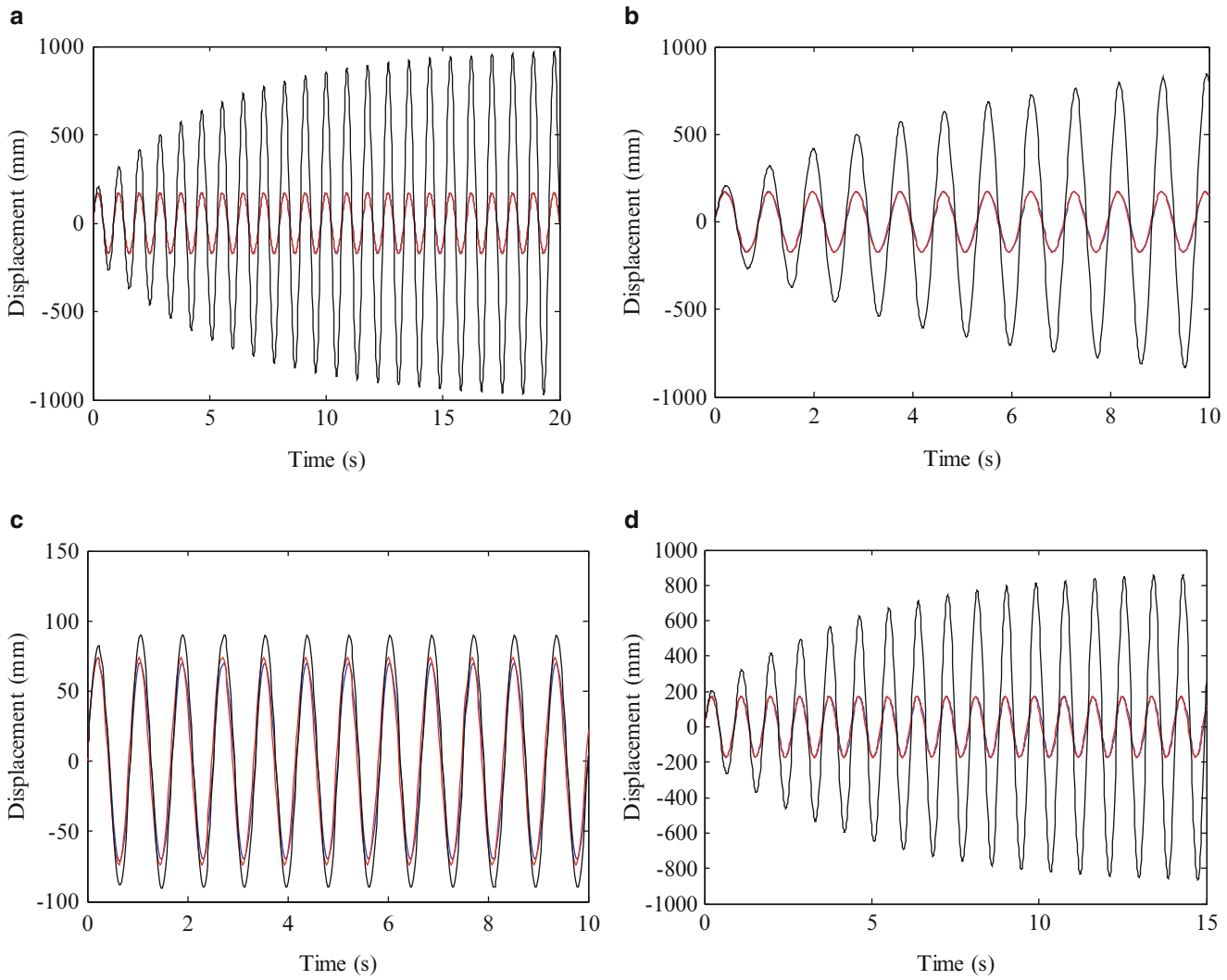

Fig. 8.3 Response of the resonant-excited system with $F = 50N$ for (**a**) $\varepsilon = 0.05$ and $\delta = 0$ (**b**) $\varepsilon = 0.05$ and $\delta = 1$ (**c**) $\varepsilon = 0.5$ and $\delta = 1$ (**d**) $\varepsilon = 0.05$ and $\delta = 2$: (*red line*) approximate analytical solution of the system with the NDD damper; (*blue line*) numerical solution of the system with the NDD damper; (*dark line*) analytical solution of the system with the linear damper

the system using the NDD damper. In the system with the linear damper; not only an undesired significant higher force is transmitted to the base but also the traditional damper is unable to provide the system with the effective amplitude reduction compared to the NDD damper.

In Fig. 8.6 the damping force versus time is shown for the first four cases given in Table 8.1. It is observed that the NDD damper provides a higher damping force and keeps the amplitude far more limited than the traditional damper while the system is excited with a resonant force. In addition, it is worthwhile to note that in Fig. 8.6c, in which the vibration amplitude is small compared to the other cases, the damping force of the NDD damper gets close to the linear damper. This is due to the fact that small amplitudes weaken of the higher powers of u in Eq. (8.6). Therefore, the damping coefficient of the NDD damper gets closer to the linear damper for the small displacements.

To study the effect of increasing the deviation factor δ, the displacement of the excited system for the case (5) where $\delta = 20$ is presented in Fig. 8.7. Figure 8.7 confirms that as the value of δ rises, the error between the approximate analytical solution given by Eq. (8.36) and the exact numerical solution increases. This is due to the fact that the scheme is elaborated for the resonant analysis, in which the value of δ is small.

As expected, when the external force's frequency gets close to the natural frequency of the system, i.e. $\delta \to 0$, the resonant excitation is more severe and consequently results in vibration with higher amplitude. On the contrary, increasing the difference between the external force's frequency and the natural frequency of the system causes decreasing the stationary

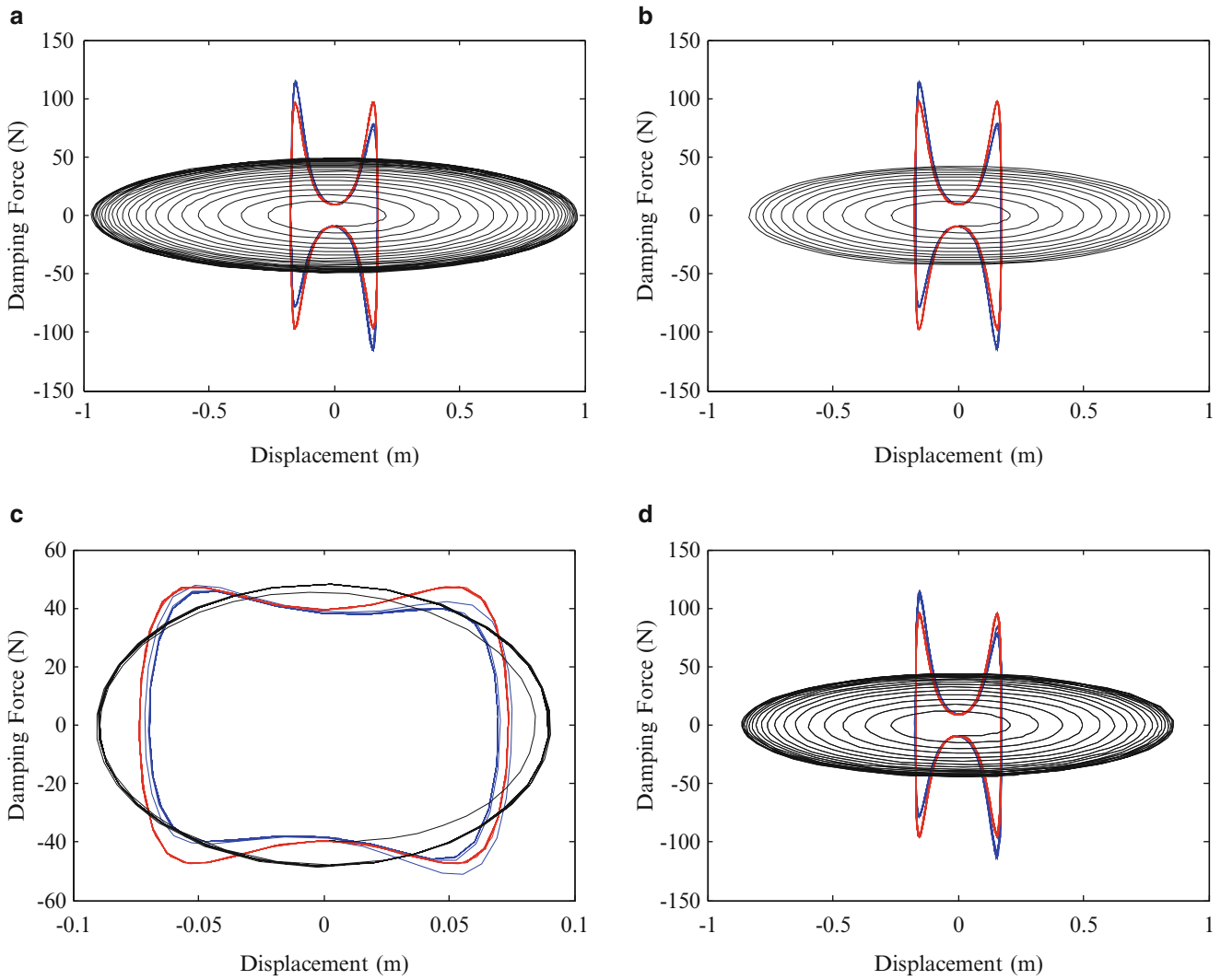

Fig. 8.4 Damping force versus displacement of the resonant-excited system with $F = 50N$ for (**a**) $\varepsilon = 0.05$ and $\delta = 0$ (**b**) $\varepsilon = 0.05$ and $\delta = 1$ (**c**) $\varepsilon = 0.5$ and $\delta = 1$ (**d**) $\varepsilon = 0.05$ and $\delta = 2$: (*red line*) damping force of the NDD damper obtained by the MSM; (*blue line*) damping force of the NDD damper obtained by the Runge–Kutta method; (*dark line*) damping force of the linear damper

amplitude response of the excited system. For the case (5) with $\delta = 20$, the response of the system with the NDD damper reaches its stationary amplitude of 168 mm, which is smaller than the stationary amplitude of the case (1) with $\delta = 0$ and case (2) with $\delta = 1$.

8.7 Conclusion

The resonant vibration analysis of a mass-spring system equipped with the nonlinear displacement-dependent (NDD) damper was studied in this paper. The governing equation of the excited system was derived for the external force with a frequency closed to the natural frequency of the system. To obtain the forced-resonant response of the system, the approximate analytical solution algorithm was developed by the multiple scales method (MSM). The advised solution algorithm was performed for several case studies with various amounts of external force's frequencies and also verified by the numerical fourth-order Runge–Kutta method. It is found that the proposed analytical solution algorithm is able to achieve the satisfactory performance for the resonant excitation analysis. In contrast to the system with the linear damper, in which the response considerably grows in each cycle up to extremely large stationary amplitude at a long time; in the system employing the NDD damper, the amplitude of the vibration tends to its stationary value immediately. Moreover, the results

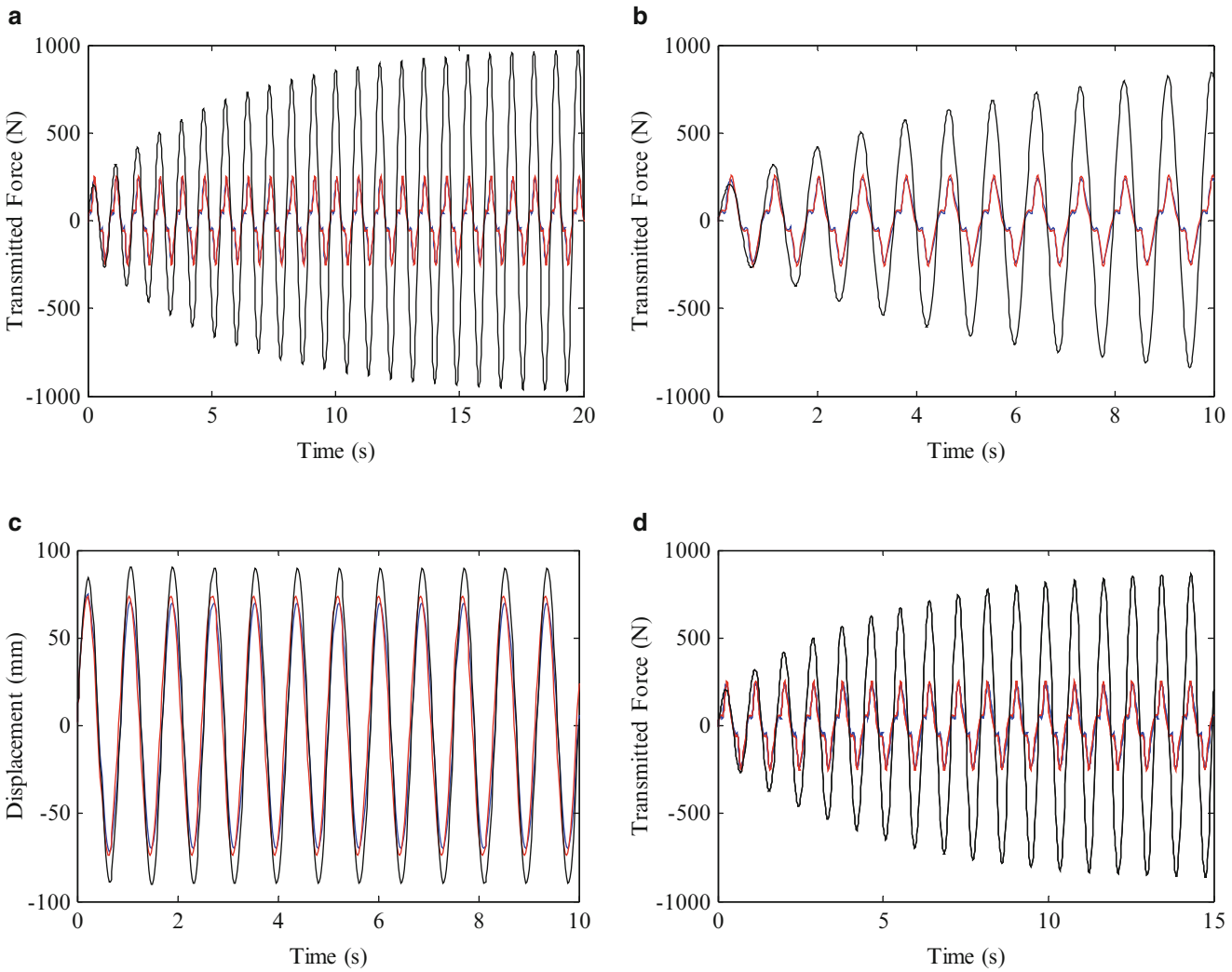

Fig. 8.5 Comparison between the transmitted force by the system in a linear system and nonlinear system with NDD damper with resonant external force as $F = 50N$ for (**a**) $\varepsilon = 0.05$ and $\delta = 0$ (**b**) $\varepsilon = 0.05$ and $\delta = 1$ (**c**) $\varepsilon = 0.5$ and $\delta = 1$ (**d**) $\varepsilon = 0.05$ and $\delta = 2$: (*red line*) approximate analytical solution of the system with the NDD damper; (*blue line*) numerical solution of the system with the NDD damper; (*dark line*) analytical solution of the system with the linear damper

confirm that utilizing the NDD damper in the resonant-excited system not only causes more vibration amplitude reduction rather than the traditional linear damper but also provides the lower force transmitted to the base compared to the linear damper, where an undesired significant higher transmitted force is produced.

A.1 Appendix

$$\begin{aligned}
\alpha_1 &= \left(\gamma^4 - 2\gamma^2 + 1\right)\lambda \\
\alpha_2 &= \left(4\gamma^4 - 4\gamma^2\right)\lambda\beta \\
\alpha_3 &= \left(6\gamma^4 - 2\gamma^2\right)\lambda\beta^2 \\
\alpha_4 &= \left(4\gamma^4\right)\lambda\beta^3 \\
\alpha_5 &= \left(\gamma^4\right)\lambda\beta^4
\end{aligned} \tag{8.41}$$

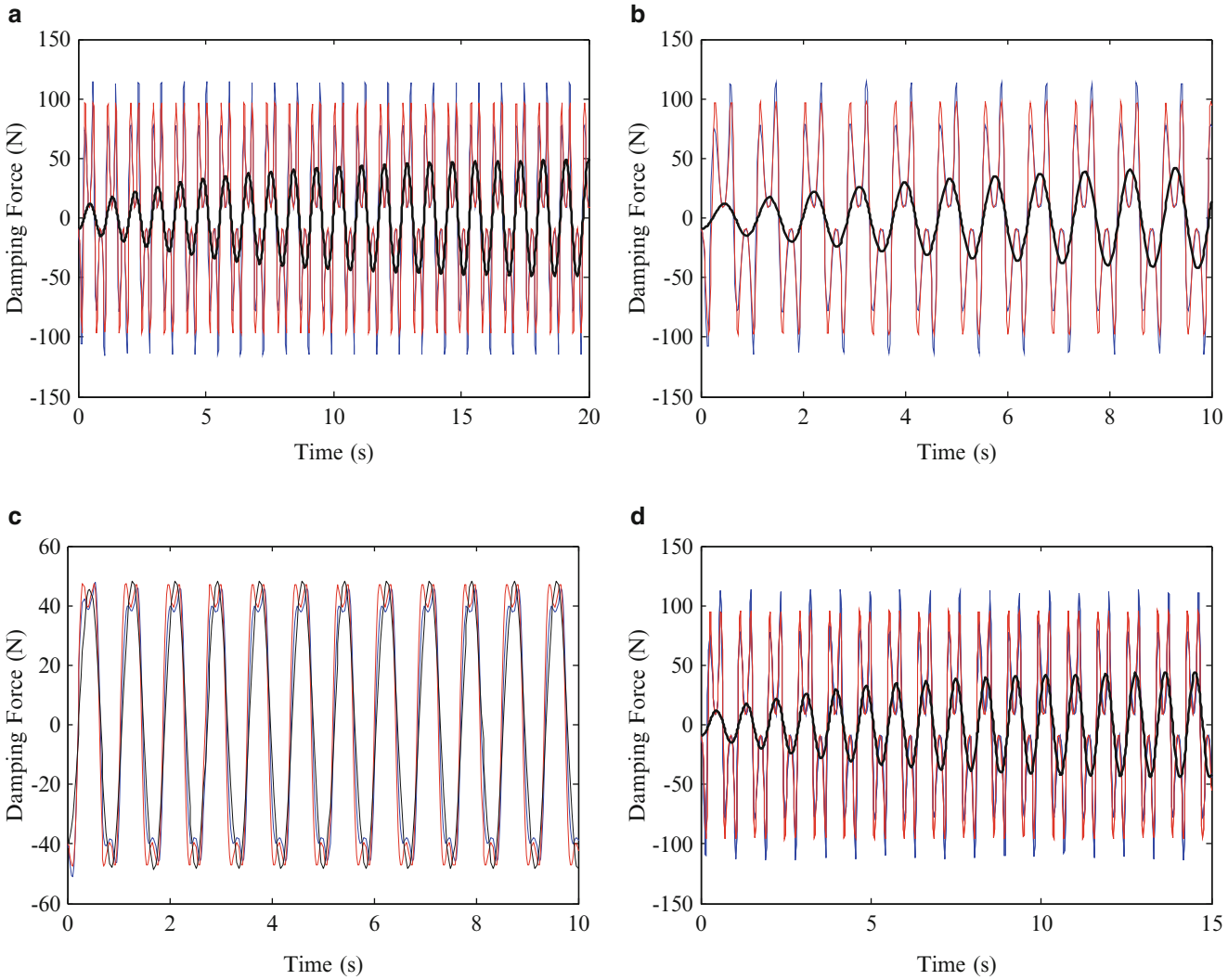

Fig. 8.6 Damping force of the resonant-excited system versus time with $F = 50N$ for (**a**) $\varepsilon = 0.05$ and $\delta = 0$ (**b**) $\varepsilon = 0.05$ and $\delta = 1$ (**c**) $\varepsilon = 0.5$ and $\delta = 1$ (**d**) $\varepsilon = 0.05$ and $\delta = 2$: (*red line*) damping force of the NDD damper obtained by the MSM; (*blue line*) damping force of the NDD damper obtained by the Runge–Kutta method; (*dark line*) damping force of the linear damper

$$\begin{aligned} A_2 &= \frac{\frac{F}{k_s}}{\sqrt{\left(1-\left(\frac{\Omega}{\omega_n}\right)^2\right)^2+\left(2\zeta\frac{\Omega}{\omega_n}\right)^2}} \\ \varphi &= \tan^{-1}\left(\frac{2\zeta\frac{\Omega}{\omega_n}}{1-\left(\frac{\Omega}{\omega_n}\right)^2}\right) \end{aligned} \tag{8.42}$$

$$\begin{aligned} \beta_1 &= \frac{(4\gamma^4-4\gamma^2)\beta}{(\gamma^4-2\gamma^2+1)} \\ \beta_2 &= \frac{(6\gamma^4-2\gamma^2)\beta^2}{(\gamma^4-2\gamma^2+1)} \\ \beta_3 &= \frac{4\gamma^4\beta^3}{(\gamma^4-2\gamma^2+1)} \\ \beta_4 &= \frac{\gamma^4\beta^4}{(\gamma^4-2\gamma^2+1)} \end{aligned} \tag{8.43}$$

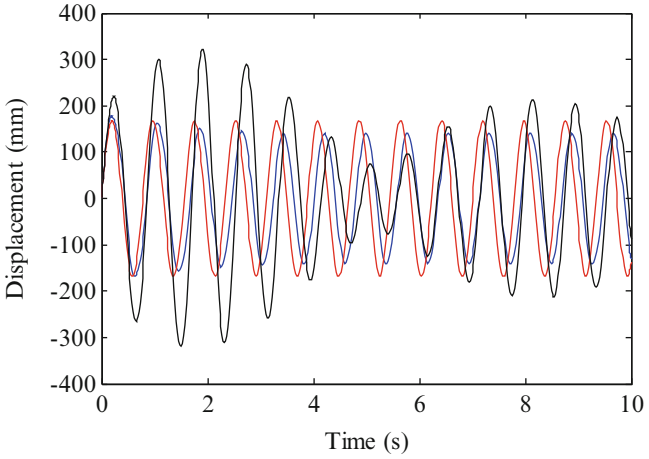

Fig. 8.7 Response of the system to the non-resonant excitation with $F = 50$ N for $\varepsilon = 0.05$ and $\delta = 20$: (*red line*) approximate analytical solution of the system with the NDD damper; (*blue line*) numerical solution of the system with the NDD damper; (*dark line*) analytical solution of the system with the linear damper

$$\begin{aligned}
\Delta_3 &= \beta_1 A^3 + 3\beta_2 A^4 \overline{A} + 28\beta_4 A^6 \overline{A}^3 + 9\beta_3 A^5 \overline{A}^2 \\
\Delta_5 &= \beta_2 A^5 + 5\beta_3 A^6 \overline{A} + 20\beta_4 A^7 \overline{A}^2 \\
\Delta_7 &= \beta_3 A^7 + 7\beta_4 A^8 \overline{A} \\
\Delta_9 &= \beta_4 A^9
\end{aligned} \tag{8.44}$$

References

1. De Silva, C.W.: Vibration: Fundamentals and Practice, 2nd edn. CRC Press, Boca Raton (2006)
2. Rao, S.S.: Mechanical Vibrations, 4th edn. Prentice-Hall, Englewood Cliffs (2004)
3. Tomson, W.T., Diloon, D.M.: Theory of Vibration with Applications, 5th edn. Nelson Thornes Ltd, Cheltenham (1998)
4. Jang, H.K.: Design guideline for the improvement of dynamic comfort of a vehicle seat and its application. Int. J. Automot. Technol. **6**, 383–390 (2005)
5. Yang, B.S., Choi, S.P., Kim, Y.C.: Vibration reduction optimum design of a steam-turbine rotor-bearing system using a hybrid genetic algorithm. Struct. Multidiscip. Optim. **30**, 43–53 (2005)
6. Asl, M.E., et al.: Predicting the vibration response in subcomponent testing of wind turbine blades. In: Allemang, R. (ed) Special Topics in Structural Dynamics, vol. 6, pp. 115–123. Springer International Publishing (2015)
7. Gibanica, M., et al.: Spread in modal data obtained from wind turbine blade testing. In: Mayes, R., Rixen, D., Allen, M. (eds.) Topics in Experimental Dynamic Substructuring, vol. 2, pp. 207–215. Springer, New York (2014)
8. Museros, P., Alarcon, E.: Influence of the second bending mode on the response of high-speed bridges at resonance. J. Struct. Eng. **131**, 405–415 (2005)
9. Jalili, N., Knowles, D.W.: Structural vibration control using an active resonator absorber: modeling and control implementation. Smart Mater. Struct. **13**, 998–1005 (2004)
10. Ilbeigi, S., Chelidze, D.: Model order reduction of nonlinear Euler-Bernoulli beam. In: Nonlinear Dynamics, vol. 1, pp. 377–385. Springer International Publishing (2016)
11. Nasiri, N., Ilbeigi, S., Nazari, F., Asmar, B., Karimi, M., Baghalian, S.: Comparison of radial basis function and back-error propagation neural networks for crack detection in variable cross-section beams (2012)
12. Kazemi, M.A., et al.: Detection of multiple cracks in beams using particle swarm optimization and artificial neural network. In: 4th International Conference on Modeling, Simulation and Applied Optimization (ICMSAO). IEEE (2011)
13. Abolbashari, M.H., Nazari, F.: A multi-crack effects analysis and crack identification in functionally graded beams using particle swarm optimization algorithm and artificial neural network. Struct. Eng. Mech. **51**, 299 (2014)
14. Aminpour, H., Nazari, F., Baghalian, S.: Applying artificial neural network and wavelet analysis for multiple cracks identification in beams. Int. J. Veh. Noise Vib. **8**(1), 51–59 (2012)
15. Nazari, F., Abolbashari, M.H., Hosseini, S.M.: Three dimensional natural frequency analysis of sandwich plates with functionally graded core using hybrid meshless local Petrov-Galerkin method and artificial neural network. Comput. Model. Eng. Sci. **105**(4), 271–299 (2015)
16. Nazari, F., Abolbashari, M.H.: Double cracks identification in functionally graded beams using artificial neural network. J. Solid Mech. **5**(1), 14–21 (2013)

17. Shobeiri, V.: Topology optimization using bi-directional evolutionary structural optimization based on the element-free Galerkin method. Eng. Optim. **48**(3), 380–396 (2016)
18. Karimi, M., Jahanpour, J., Ilbeigi, S.: A novel scheme for flexible NURBS-based C2 PH Spline Curve contour following task using Neural Network. Int. J. Precis. Eng. Manuf. **15**(12), 2659–2672 (2014)
19. Love, J.S., Tait, M.J.: Non-linear multimodal model for tuned liquid dampers of arbitrary tank geometry. Int. J. Non-Linear Mech. **46**, 1065–1075 (2011)
20. Afsharfard, A., Farshidianfar, A.: Design of nonlinear impact dampers based on acoustic and damping behavior. Int. J. Mech. Sci. **65**(1), 125–133 (2012)
21. Butcher, E.A.: Clearance effects on bilinear normal mode frequencies. J. Sound Vib. **224**, 305–328 (1999)
22. Metallidis, P., Natsiavas, S.: Vibration of a continuous system with clearance and motion constraints. Int. J. Non-Linear Mech. **35**, 675–690 (2000)
23. Pun, D., Lau, S.L., Liu, Y.B.: Internal resonance of an L-shaped beam with a limit stop I, free vibration. J. Sound Vib. **193**, 1023–1035 (1996)
24. Pun, D., Lau, S.L., Liu, Y.B.: Internal resonance of an L-shaped beam with a limit stop II, forced vibration. J. Sound Vib. **193**, 1037–1047 (1996)
25. Moradi, H., Vossoughi, G., Movahhedy, M.R., Ahmadian, M.T.: Forced vibration analysis of the milling process with structural nonlinearity, internal resonance, tool wear and process damping effects. Int. J. Non-Linear Mech. **54**, 22–34 (2013)
26. Perepelkin, N.V., Mikhlin, Y.V., Pierre, C.: Non-linear normal forced vibration modes in systems with internal resonance. Int. J. Non-Linear Mech. **57**, 102–115 (2013)
27. Ilbeigi, S., Jahanpour, J., Farshidianfar, A.: A novel scheme for nonlinear displacement-dependent dampers. Nonlinear Dyn. **70**, 421–434 (2012)
28. Dixon, J.C.: The Shock Absorber Handbook, 2nd edn. Wiley, Chichester (2007)
29. Eslaminasab, N.: Development of a semi-active intelligent suspension system for heavy vehicles. Ph.D. Thesis, University of Waterloo, Canada (2008)
30. Zhou, N., Liu, K.: A tunable high-static-low-dynamic stiffness vibration isolator. J. Sound Vib. **329**, 1254–1273 (2010)
31. Wang, W.L., Xu, G.X.: Fluid formulae for damping changeability conceptual design of railway semi-active hydraulic dampers. Int. J. Non-Linear Mech. **44**, 809–819 (2009)
32. Dong, X.-M., Yu, M., Liao, C.-R., Chen, W.-M.: Comparative research on semi-active control strategies for magnet-rheological suspension. Nonlinear Dyn. **59**(433–453) (2010)
33. Song, X., Ahmadian, M.: characterization of semi-active control system dynamics with magneto-rheological suspensions. J. Vib. Control **16**(10), 1439–1463 (2010)
34. Go, C.-G., Sui, H., Shih, M.-h, Sung, W-P.: A linearization model for the displacement dependent semi-active hydraulic damper. J.Vib. Control **16**(14), 219–2214 (2010)
35. Preumont, A.: Vibration Control of Active Structures. Kluwer Academic Publishers, Dordrecht. EBook ISBN: 0-306-48422-6 (2002)
36. Crosby, M.J., Karnopp, D.C.: The active damper—a new concept for shock and vibration control. Shock Vib. Bull. **43**(4), 119–133 (1973)
37. Ahmadian, M.: On the isolation properties of semiactive dampers. J. Vib. Control **5**(2), 217–232 (1999)
38. Simon, D.E.: Experimental evaluation of semiactive magneto-rheological primary suspensions for heavy truck applications. Ph.D. Thesis, Virginia Tech (2000)
39. Venkatesan, C., Krishnan, R.: Harmonic response of a shock mount employing dual-phase damping. J. Sound Vib. **40**(3), 409–413 (1975)
40. Jackson, G.W.: Fundamentals of the Direct Acting Shock Absorber. SAE paper 37R, National Passenger Car Body and Materials Meeting, Detroit, (1959)
41. Puydak, R.C., Auda, R.S.: Designing to achieve optimum dynamic properties in elastomeric cab and body mounts. SAE 660439 (and SAE Transactions V75), (1966)
42. Lewitske, C., Lee, P.: Application of elastomeric components for noise and vibration isolation in the automotive industry. SAE Paper 2001-01-1447 (2001)
43. Fukushima, N., Hidaka, K., Iwata, K.: Optimum characteristics of automotive shock absorbers under various driving conditions and road surfaces. JSAE Rev. 62–69 (1983)
44. Young, D.W.: Aircraft Landing Gears. Proc. I. Mech. E. **200**(D2), 75–92 (1986)
45. Etman, L.F.P., Vermeulen, R.C.N., Van Heck, J.G.A.M., Schoofs, A.J.G., Van Campen, D.H.: Design of a stroke dependent damper for the front axle suspension of a truck using multibody system dynamics and numerical optimization. Veh. Syst. Dyn. **38**, 85–101 (2002)
46. Komamura, S., Mizumukai, K.: History of shock absorbers. Automob. Technol. **41**(1), 126–131 (1987) (in Chinese)
47. Lee, C.-T., Moon, B.-Y.: Study on the damping performance characteristics analysis of shock absorber of vehicle by considering fluid force. J. Mech. Sci. Technol. **19**(2), 520–528 (2005)
48. Lee, C.-T., Moon, B.-Y.: Simulation and experimental validation of vehicle dynamic characteristics for displacement-sensitive shock absorber using fluid-flow modeling. Mech. Syst. Sig. Process. **20**, 373–388 (2006)
49. Hundal, M.S.: Impact absorber with two-stage variable area orifice hydraulic damper. J. Sound Vib. **50**(2), 195–202 (1977)
50. Haque, M.M., Ahmed, A.K.W., Sankar, S.: Simulation of displacement sensitive non-linear dampers via integral formulation of damping force characterization. J. Sound Vib. **187**, 95–109 (1995)
51. Farjoud, A., Ahmiadian, M., Craft, M., Burke, W.: Nonlinear modeling and experimental characterization of hydraulic dampers: effects of shim stack and orifice parameters on damper performance. Nonlinear Dyn. **67**(2), 1437–1456 (2012)
52. Guo, P.F., Lang, Z.Q., Peng, Z.K.: Analysis and design of the force and displacement transmissibility of nonlinear viscous damper based vibration isolation systems. Nonlinear Dyn. **67**(4), 2671–2687 (2012)
53. Peng, Z.K., Lang, Z.Q., Billings, S.A.: Resonance and resonant frequencies for a class of nonlinear systems. J. Sound Vib. **300**, 993–1014 (2007)
54. Asfar, K.R., Masoud, K.K.: Damping of parametrically excited single-degree-of-freedom systems. Int. J. Non-Linear Mech. **29**, 421–428 (1994)

55. Bugra, H., Ertas, B.H., Luo, H.: Nonlinear dynamic characterization of oil-free Wire mesh dampers. Gas Turbines Power **130**(3), 032503 (2008)
56. Main, J.A., Jones, N.P.: Analysis and design of linear and nonlinear dampers for stay cables. In: Proceedings Fourth International Symposium on Cable Dynamics, Montreal, Canada, AIM, 2001
57. Diotallevi, P.P., Landi, L., Dellavalle, A.: Simplified design methodology for systems equipped with non-linear viscous dampers. In: The 14th World Conference on Earthquake Engineering, Beijing, China, 2008
58. Ilbeigi, S., Jahanpour, J., Farshidianfar, A.: Forced vibration analysis of a system equipped with the nonlinear displacement-dependent (NDD) damper. Article in press in Scientia Iranica, Int. J. Sci. Technol.
59. Nayfeh, A.H., Mook, D.T.: Nonlinear Oscillations. Wiley, New York (1979)
60. Nayfeh, A.H.: Perturbation Methods. Wiley, New York (1973)
61. Alijania, F., Amabilib, M., Bakhtiari-Nejada, F.: On the accuracy of the multiple scales method for non-linear vibrations of doubly curved shallow shells. Int. J. Non-Linear Mech. **46**, 170–179 (2011)